

Star Cluster Survival in Star Cluster Complexes under Extreme Residual Gas Expulsion

M. Fellhauer and P. Kroupa

Sternwarte University of Bonn, 53121 Bonn, Germany

mike,pavel@astro.uni-bonn.de

ABSTRACT

After the stars of a new, embedded star cluster have formed they blow the remaining gas out of the cluster. Especially winds of massive stars and definitely the on-set of the first supernovae can remove the residual gas from a cluster. This leads to a very violent mass-loss and leaves the cluster out of dynamical equilibrium. Standard models predict that within the cluster volume the star formation efficiency (SFE) has to be about 33 per cent for sudden (within one crossing-time of the cluster) gas expulsion to retain some of the stars in a bound cluster. If the efficiency is lower the stars of the cluster disperse mostly.

Recent observations reveal that in strong star bursts star clusters do not form in isolation but in complexes containing dozens and up to several hundred star clusters, i.e. in super-clusters. By carrying out numerical experiments for such objects placed at distances ≥ 10 kpc from the centre of the galaxy we demonstrate that under these conditions (i.e. the deeper potential of the star cluster complex and the merging process of the star clusters within these super-clusters) the SFEs can be as low as 20 per cent and still leave a gravitationally bound stellar population. Such an object resembles the outer Milky Way globular clusters and the faint fuzzy star clusters recently discovered in NGC 1023.

Subject headings: stars: formation — galaxies: starburst — galaxies: star clusters — globular clusters: general — methods: N-body simulations

1. Introduction

Star clusters form out of collapsing cloud clumps in molecular clouds (Tilley & Pudritz 2004). These collapses are triggered by turbulent fragmentation of clouds and their clumps (MacLow & Klessen 2004). The clumps are observed to be aligned in filamentary structures that can be reproduced by supersonic turbulent simulations and they contain many cores (Burkert & Bodenheimer

2000; Klessen & Burkert 2001). Each core forms a single star or a binary. The mass function found for these cores is essentially the same as the initial mass function of the stars (Johnstone et al. 2000). While the star formation efficiency (SFE; i.e. the fraction of gas which ends up in the star(s)) in these cores is high, the overall SFE measured over the whole molecular cloud is very low, of the order of a few per cent (Clark & Bonnell 2004), and ≤ 40 per cent in cluster forming clumps (i.e. embedded star clusters; Lada & Lada 2003).

The remaining gas does not stay in the newborn star cluster but is driven outwards by stellar feedback. In embedded clusters containing more than a few hundred stars the feedback consists of photo-ionising radiation, the winds of high-mass stars and finally the on-set of the first supernova explosions (Goodwin 1997). For such clusters the feedback energy can easily be sufficient to unbind the gas leading to a gas expulsion phase which is rather short, comparable to the crossing time of the star cluster. Pictures of young massive star clusters, for example in the central region of the Antennae (NGC 4038/4039; Whitmore et al. 1999), reveal that they are already surrounded by H- α bubbles stemming from the gas which was blown out of the star cluster. It has been shown that these star clusters can be as young as 5–6 Myr. The outflow velocities of the gas has been measured to be 25–30 kms^{-1} (Whitmore et al. 1999), which corresponds to gas-evacuation times of 0.2 Myr for cluster radii of 4 pc. This is comparable to the crossing time of a $10^5 M_{\odot}$ cluster.

As a result of this strong and rapid mass-loss the star cluster is left out of virial equilibrium. The velocities of the stars are too high for the reduced mass of the star cluster. So even more mass is lost when stars escape from the star cluster. This may finally lead to the complete dissolution of the cluster. But if the star formation efficiency is as high as 33 per cent or above, a small bound core remains (Goodwin 1997; Boily & Kroupa 2003a,b) and today we therefore understand the formation of low-mass, Pleiades-type clusters (Kroupa et al. 2001). Geyer & Burkert (2001) argue that the SFE has to be larger than 50 per cent to get a bound core but if the stars have almost no initial velocity dispersion then 10 per cent could be enough. This means that the measurement of the initial velocity distribution in newborn embedded star clusters will be crucial to find out if and how star clusters survive.

As seen in the beautiful HST images of the central region of the Antennae galaxies (Whitmore et al. 1999), star clusters in strong star bursts do not form in isolation but rather in star cluster complexes. These are confined regions of several hundred parsecs containing dozens and up to hundreds of young massive star clusters (Kroupa 1998; Zhang & Fall 1999).

Following the arguments of Kroupa (1998) these star cluster complexes are bound entities and should be close to virial equilibrium. Even though they are quite young (in the Antennae ≤ 10 Myr) they should be already more dispersed and not centrally concentrated anymore if they are unbound, or almost all clusters should be merged in the centre if they are sub-virial. Until now there is no observational measurement of the velocity dispersion in the cluster complex available. Observers

have only measured the velocity dispersions of the star clusters. However, the difference in radial velocity of two star clusters in the same cluster complex ($\approx 20 \text{ kms}^{-1}$) is in good agreement with the assumption that the complex is a bound entity.

In this paper we investigate the birth of massive star clusters in such extreme environments. Our aim is to understand what rôle star cluster complexes, with their collective potential and the ability for the star clusters to merge with each other on short timescales (Fellhauer et al. 2002), have for retaining a bound core.

In the next section we describe the code we are using and the setup of our models. Then we present our results followed with a discussion.

2. Setup

We use the particle-mesh code SUPERBOX (Fellhauer et al. 2000) which allows us to keep track of many objects in one simulation. This code has a hierarchical grid structure where the high-resolution sub-grids stay focused on the simulated objects while they move through the simulation area. Each grid contains 64^3 grid-cells in this simulation. This enables us to resolve the forces between the star clusters as well as the forces within a star cluster correctly. We choose the grids of SUPERBOX in a way that the innermost grid-level with the highest resolution (1.0 pc per cell) covers each star cluster, while the medium resolution grids (5.0 pc per cell) have the size of the star cluster complex. Finally the outermost grid (500 pc per cell) covers the whole orbit of the star cluster complex around the host galaxy. The time-step of our simulations was chosen to be 0.1 Myr which ensures enough time-steps per crossing time of the single clusters (24 per crossing-time) and of the dense star cluster complex (59 per crossing-time). The CPU time needed was about 96 sec per time-step, or about 10 days for a 1 Gyr simulation (on standard desktop PCs).

The single star clusters are represented by Plummer spheres with a Plummer radius of 4 pc and a cut-off radius of 25 pc. Each cluster has a mass of $10^5 M_{\odot}$ initially, a crossing time of 2.4 Myr and is represented with 100,000 particles.

20 of these clusters are placed in a star cluster complex which is modelled again as a Plummer distribution (i.e. positions and velocities according to the Plummer distribution function), now with the star clusters as 'particles'. This Plummer distribution is given a Plummer radius of 20 pc, a cut-off radius of 100 pc, a crossing time of 5.9 Myr and a characteristic velocity dispersion of 11.25 kms^{-1} . This is a very dense configuration which will lead to a fast merging of the star clusters into one massive merger object, if mass-loss is not taken into account. It also implies that the star clusters as well as the star cluster complex is in virial equilibrium before the gas-expulsion.

The initial conditions of our cluster complex are comparable to the cluster complexes in the central regions of the Antennae galaxies only in a qualitative way. However, cluster complexes are not only found in the central star bursts of interacting galaxies like the Antennae, but also in tidal tails (e.g. Tadpole galaxies, Stephan’s Quintet and also the Antennae) and in more quiescent galaxies like NGC 6946 (Larsen et al. 2002). They cover a wide range in total mass (10^6 – $10^8 M_{\odot}$ or even higher) and central concentrations. The knots in the Antennae galaxies are much more massive than our initial conditions and also cover a larger area. Nevertheless the density distribution there is exponential in the inner part and has a power-law drop off in the outer part (Whitmore et al. 1999). Our models, especially after the merging of the first few clusters show exactly the same behaviour (Fellhauer & Kroupa 2002b). In Fig. 1 we compare the surface-brightness profiles of our models (measured at different times using mass-to-light ratios from a single stellar population computed with Starburst99 (Leitherer et al. 1999)) with the profiles found by Whitmore et al. (1999) for three super-clusters in the Antennae.

A detailed discussion about merging time-scales, the effect of tides on the formation of the merging object as well as a discussion of the properties of the merger objects (without mass-loss) in general is found in our previous papers (Fellhauer et al. 2002; Fellhauer & Kroupa 2002a,b).

For our simulations in this project we choose a very dense configuration for the star cluster complex. In this case the merging time-scale becomes comparable to the mass-loss time-scale and the effect of the cluster complex on retaining stars forming an extended merger object should be strongest. The SFE is varied over a wide range to investigate the influence of this new environment theoretically.

The mass-loss due to gas-expulsion is modelled by all particles losing a fraction of their mass linearly over a crossing-time of the single star cluster. We consider two mass-loss models. In the coeval model every star cluster starts immediately and at the same time to lose mass and in the delayed model the star clusters start to lose their mass randomly during the first crossing time of the super-cluster. While in the coeval cases the star formation rates (SFR) range from 0.08 to $0.8 M_{\odot}/\text{yr}$ (all stars form within a crossing time of a individual cluster) the delayed models imply SFRs from 0.03 to $0.3 M_{\odot}/\text{yr}$ (the stars form within the crossing time of the star cluster complex). Using the crossing time of the cluster complex as the maximum time delay between the start of the star formation of two individual clusters is in agreement with the analysis of Efremov & Elmegreen (1998) and their time difference–separation–relation (see their fig. 8).

The star cluster complex orbits circularly at a distance of 10 kpc around an analytical galactic potential with a flat rotation curve of 220 km s^{-1} .

3. Results

First we checked if our approach gives the same results on isolated single clusters as published before by evaluating the remaining bound mass of an isolated cluster after 1 Gyr. The bound mass is computed by calculating the total energy of each particle at each time step. If the kinetic energy of the particle with respect to the star cluster centre exceeds the potential energy derived from the grid-based potentials of SUPERBOX the particle is regarded as being unbound.

The results, shown in Tab. 1 and Fig. 2, agree with the numbers in the literature (Goodwin 1997; Boily & Kroupa 2003a,b). If the SFE is higher than 33 per cent a small bound core survives. We get a star cluster which retains more than 50 per cent of its stellar mass if the SFE is about 40–50 per cent. For each SFE value we performed three simulations with different random realisations. The results of the individual realisations all agreed to better than one per cent.

As a next step we performed simulations with 20 star clusters as described above. In Tab. 2 we give the number of star clusters which have merged (M), the number of clusters which completely dissolve (D), and the number of star clusters which survive as single entities after leaving the potential of the star cluster complex (S). For the bound mass fraction of the merger object (f_b^M) we count the merged clusters as well as the completely dissolved ones. The mass of the escaped and surviving star clusters (i.e. that have neither dissolved nor merged) is not taken into account. If one or more star clusters survive we calculate their own bound mass fraction (f_b^S). The resulting bound mass fractions are shown in Fig. 3. Again the values are taken after 1 Gyr of evolution.

As a first result of our investigation we find that, in contrast to the isolated cluster case, the resulting bound mass fractions have a wide spread. Even though we just perform one simulation per parameter set we sometimes find more than one merger object or more than one surviving star cluster. In those cases a one sigma deviation can be as high as 10 per cent in f_b . This can be explained by the additional but random destructive tidal forces between the star clusters. Almost all clusters which do not end up inside the merger object have a smaller bound mass than in the isolated case. There are even star clusters dissolving completely when the SFE is 70 per cent. On the other hand there are rare cases where single clusters escape and survive even at low star formation efficiencies. Two single clusters escape and survive the coeval simulation with a SFE of 30 per cent. We analyse one of these surviving star cluster in a sub-section below (Sect. 3.2).

The merger objects in our simulations survive with very low SFE. In the delayed gas expulsion simulations we find a surviving merger object at a SFE of only 20 per cent. We followed the evolution of the merger object for 10 Gyr to see if it survives and which properties it has (Sect. 3.1).

Generally speaking the building up of a merger object with its deeper potential well favours the survival of a bound object that retains more of its stars than an isolated single cluster would, as long as the SFE is below 60 per cent (Fig 3). If the SFE is higher destructive processes during

the merging process lead to a mass-loss, i.e. stars that are expelled as a result of the kinetic energy surplus produced during the merging of the clusters (the stars are then found in the tidal tails), leaving the remaining object with a smaller bound mass fraction than the star clusters would have had if they would have formed in isolation.

However, as a major result we find that cluster formation in complexes allows star clusters to survive even if the SFE is as low as 20 per cent. In a dense star cluster complex the crossing time of the star clusters through the super-cluster, and therefore the merging time-scale, is short enough that some star clusters have already merged before they expel their gas. The much deeper potential wells of these merger objects are able to retain the stars more effectively than isolated clusters would.

To show the influence of the richness of the star cluster complex we performed one comparison simulation, where we placed an extended star cluster complex (Plummer-radius of 250 pc and a cut-off radius of 1.25 kpc) on an eccentric orbit far out (apogal: 100 kpc; perigal: 80 kpc). The complex contains 32 star clusters and has a total mass of $8.8 \cdot 10^6 M_{\odot}$ or $2.64 \cdot 10^6 M_{\odot}$ after the delayed gas-expulsion (SFE= 0.3). This also implies a low star formation rate of only $0.02 M_{\odot}/\text{yr}$. The crossing-time of this complex is long ($T_{\text{cr}} = 124 \text{ Myr}$) compared to the gas-expulsion time, which happens on the time-scales of the crossing-time of the single clusters. In this simulation only two star clusters merge and two get dissolved. All the other star clusters survive but get dispersed, because the potential of the complex is not deep enough to retain the star clusters after gas-expulsion. Also the merging time-scale which is of the order of a few crossing-times of the complex is too long to prevent the star clusters from leaving the complex. Still, as said above, almost all clusters survive and retain about 29 per cent of their initial mass in stars after one Gyr. A magnitude-spaced contour-plot of this simulation is shown in Fig 4.

3.1. Merger Object at a SFE of 20 per cent

In the randomly delayed gas expulsion experiment the merging process takes place faster than the dissolution of the star clusters. This means there is already a massive merger object with a deeper potential well when the major part of the gas expulsion occurs. This enables the object to retain a higher fraction of the stars bound to each other.

We followed the evolution of this object for 10 Gyr. After a rapid mass loss during the first few hundred Myr (Fig. 5, right panel) the merger object survives and hosts finally (after 10 Gyr) about 14 per cent of the initially formed stars. This amounts in our case to a mass of $5.42 \cdot 10^4 M_{\odot}$, or, adopting a typical mass-to-light ratio for globular clusters of 3, to an absolute V-band magnitude of -5.77 . After a first expansion phase during the first few dozens of Myr the expansion is halted

by the self-gravity of the object and the particles recollapse again. It takes a few hundred Myr until the object settles down but afterwards it loses mass and shrinks further only slowly (Fig. 5).

By 10 Gyr the object does not look like an ‘ordinary’ globular cluster but rather like one of the faint fuzzy star clusters (Larsen & Brodie 2000). It has no dense core and a large effective radius of about 13 pc. The half mass radius of the object is 18.2 pc (Fig. 5 left panel). We fit a King profile to the surface density profile with a core radius of 12.8 ± 0.2 pc and a central surface density of $124.8 \pm 0.8 M_{\odot} \text{pc}^{-2}$. This translates to $22.4 \text{ mag.arcsec}^{-2}$ (again in the V -band) taking a mass-to-light ratio of 3. The tidal radius is 56.5 pc (Fig. 6 left panel). The velocity dispersion profiles can be fitted with an exponential profile with a central value of 1.6 kms^{-1} and an effective radius of 80 pc for the line-of-sight velocity dispersions, and $3.06 \pm 0.02 \text{ kms}^{-1}$ and 66.1 ± 2.2 pc for the three dimensional velocity dispersion. We also find a steep rise in the dispersions among unbound particles outside the tidal radius. These extra tidal stars are mainly located in tidal arms leading and trailing the object.

3.2. Surviving Star Cluster at SFE of 30 per cent

In the coeval simulation with a SFE of 30 per cent we find two single clusters which do not merge and do not dissolve. They get kicked out of the potential of the star cluster complex and retain 20 per cent of their stars bound at $t = 1$ Gyr. In the left panel of Fig. 7 the bound mass fraction of one of them is shown. Clearly visible is a steep increase of the bound mass fraction at about 3 Myr. At this time the star cluster has a close encounter with another star cluster and gets shot out of the cluster complex. This event shocked the particle distribution and prevented otherwise unbound particles from gaining too much energy and becoming unbound. In the right panel of Fig. 7 we see that this event is almost invisible in the Lagrangian radii of the particles. They still keep on expanding. The turning point when the remaining particles contract again (due to their self-gravity) to form the surviving object is much later (at about 50 Myr). After that the object evolves and loses mass only slowly thereby shrinking in size until final dissolution.

By one Gyr the star cluster has a bound mass fraction of 19 per cent which amounts to $5.8 \cdot 10^3 M_{\odot}$. The bound particles form a core surrounded by a halo of unbound particles. The core has a tidal radius of about 27 pc. The shape of the surface brightness profile is best fitted with a King profile in the centre with a core radius of 20.6 pc and a power-law in the outer part and extends further than the tidal radius as shown in the left panel of Fig. 8. The line-of-sight velocity dispersion has an exponential shape out to the tidal radius and rises beyond this point due to the surrounding unbound particles.

To follow the future evolution of less massive objects like this cluster one would definitely

need a direct N-body code to account for internal evolution caused by two-body relaxation effects. Nevertheless as shown in Fig 7 (right panel) with our code which suppresses two-body relaxation completely the dissolution time is about 3 Gyr. Comparing our result with simulations by Baumgardt & Makino (2003) (their fig. 3) our result is very similar to that obtained from their more appropriate simulation (dissolution time 3.5 Gyr).

4. Discussion and Conclusion

In the isolated case our models are able to reproduce the standard value for the SFE to retain a bound object after gas-expulsion. The critical SFE beyond which a few per cent of bound stars are retained is 33 per cent (for gas-expulsion within a crossing-time). The SFE which leads to an object which one can call a star cluster is about 50 per cent. These results are in excellent agreement with previous theoretical works (Goodwin 1997; Geyer & Burkert 2001) using collision-less methods and give us confidence in the correctness of our approach of treating gas expulsion. The use of collisional N-body codes reduces these values further and experiments (Kroupa et al. 2001) show a remaining bound object of size and richness of the Pleiades at a SFE of 30 per cent for an initially embedded Orion-Nebula like cluster consisting of 10^4 stars and brown dwarves.

This work has shown that, for star clusters forming in star cluster complexes, there is no clear correlation between SFE and final mass of the object. This is due to the random realisations of the star clusters inside the cluster complex leading to different individual encounter and merger histories. As a general trend we can state that this environment is able to assemble a bound object at a much lower SFE than the isolated case would predict. We find a surviving bound object at a star formation efficiency as low as 20 per cent. For low SFEs the resulting bound mass of the remaining object is on average higher than the isolated case would predict. But if the SFE is very high the destructive forces of the encounters and merging become dominant and the resulting merger objects retain a significantly lower bound mass than in the isolated case.

One reason for the ability of cluster complexes to reduce the necessary SFE for a bound object is the deeper potential well of the cluster complex which helps to retain some of the escaping stars. But another important reason is the merging of the star clusters. As already shown in previous studies (Fellhauer et al. 2002) the star clusters in dense cluster complexes merge on very short time-scales, namely a few crossing-times of the cluster complex, with a merger object visible already in the first one or two crossing times. If the complex is dense enough, i.e. its crossing-time is short and of the order of the gas-expulsion time-scale, some clusters merge and form a larger, more massive object before stars react to the gas-loss and try to escape. Within the more massive merger object they need a much higher escape velocity and more stars stay gravitationally bound and recollapse again to form a bound object. While such objects can be dense and massive enough

to survive for a Hubble time (Baumgardt 1998), they do not resemble normal globular clusters because they have rather large effective radii. They can only survive as noticeable objects in a weak tidal field and thus in the outskirts of galaxies, having been born for example in tidal tails of interacting gas-rich galaxies.

While our study is based on dense star cluster complexes as found in the central region in the Antennae (Whitmore et al. 1999), we also performed a simulation with a SFE of 30 per cent and delayed gas-expulsion placing an extended cluster complex in the outer halo region. Even though, due to the long crossing-time scales of this complex the star clusters rather disperse than merge, the environment (i.e. the deeper potential of the star cluster complex) is able to help these dispersed star clusters to survive. They still resemble bound objects retaining almost a third of their initial mass in stars even after one Gyr.

We described the further evolution of one of our merger objects (in the extreme case) with a SFE of 20 per cent in detail. The properties of this object (low mass, large effective radius) are similar to those found for the faint fuzzy star clusters in NGC 1023 (Larsen & Brodie 2000). Our objects also resemble the faint GCs in the outer MW halo (Côté et al. 2002; Harris 1997). The relaxation time of such an object amounts to ≈ 8.5 Gyr.

In one of our simulations we found an escaping and surviving single star cluster at a SFE which shouldn't allow its survival. We argued that a close encounter with another star cluster which lead to an expulsion instead of a merger was able to 'shock' the particle distribution such that the expanding and dissolution process was compensated leaving a low-mass but large, bound star cluster behind. Even though an object that small would not survive for a Hubble time due to internal two-body relaxation (Baumgardt 1998) (the relaxation time measured at $t = 1$ Gyr is 2.6 Gyr, and due to constant mass-loss is reduced to 800 Myr at $t = 3$ Gyr) one might find young or even intermediate age objects close to star-burst regions which could look like our model. Another observational counterpart regarding the physical properties might be the recently discovered (Willman et al. 2004) unusual 'globular' cluster SDSSJ1049+5103. It has a half-light radius of 23 ± 10 pc and a mass in the range of a few hundred up to a thousand solar masses. The authors argue that this cluster is either in the final stage of dissolution, which would make it a perfect counterpart to our surviving star cluster (seen at its final stage at $t = 3$ Gyr), or a very faint and low-mass dwarf spheroidal galaxy embedded in a dark matter halo.

MF thankfully acknowledges financial support through DFG-grant KR1635/5-1.

REFERENCES

- Baumgardt, H., 1998, *Å*, 330, 480
- Baumgardt, H., Makino, J., 2003, *MNRAS*, 340, 227
- Boily, C.M., & Kroupa, P., 2003, *MNRAS*, 338, 665
- Boily, C.M., & Kroupa, P., 2003, *MNRAS*, 338, 673
- Burkert, A., & Bodenheimer, P., 2000, *ApJ*, 543, 822
- Clark, P.C., & Bonnell, I.A., 2004, *MNRAS*, 347, L36
- Côté, P., Djorgovski, S.G., Meylan, G., Castro, S., & McCarthy, J.K., 2002, *ApJ*, 574, 783
- Efremov, Y.N., & Elmegreen, B.G., 1998, *MNRAS*, 299, 588
- Fellhauer, M., Kroupa, P., Baumgardt, H., Bien, R., Boily, C.M., Spurzem, R., & Wassmer, N., 2000, *New A*, 5, 305
- Fellhauer, M., Baumgardt, H., Kroupa, P., & Spurzem, R., 2002, *Cel.Mech.& Dyn.Astron.*, 82, 113
- Fellhauer, M., & Kroupa, P. 2002, *MNRAS*, 330, 642
- Fellhauer, M., & Kroupa, P. 2002, *AJ*, 124, 2006
- Geyer, M.P., Burkert, A., 2001, *MNRAS*, 323, 988
- Goodwin, S., 1997, *MNRAS*, 284, 785
- Harris, W.E., 1997, *VizieR Online Data Catalogue*, 7202, 0
- Johnstone, D., Wilson, C.D., Moriaty-Schieven, G., Joncas, G., Smith, G., Gregersen, E., & Fich, M., 2000, *ApJ*, 545, 327
- Klessen, R.S., & Burkert, A., 2001, *ApJ*, 549, 386
- Kroupa, P., 1998, *MNRAS*, 300, 200
- Kroupa, P., Aarseth, S., & Hurley, J., 2001, *MNRAS*, 321, 699
- Lada, C.J., & Lada, E.A., 2003, *ARA&A*, 41, 57
- Larsen, S.S., & Brodie, J.P. 2000, *AJ*, 120, 2938

- Larsen, S.S., Efremov, Y.N., Elmegreen, B.G., Alfaro, E.J., Battinelli, P., Hodge, P.W., & Richtler, T. 2002, *ApJ*, 567, 896
- Leitherer, C., Schaerer, D., Goldader, J.D., Delgado, R.M.G., Robert, C., Kune, D.F., de Mello, D.F., Devost, D., Heckman, T.M. 1999, *ApJS*, **123**, 3
- MacLow, M., & Klessen, R., 2004, *RvMP*, 76, 125
- Tilley, D.A., & Pudritz, R.E., 2004, *MNRAS*, 353, 769
- Whitmore, B.C., Zhang, Q., Leitherer, C., & Fall, S.M., 1999, *AJ*, 118, 1551
- Willman, B., Blanton, M.R., West, A.A., Dalcanton, J.J., Hogg, D.W., Schneider, D.P., Wherry, N., Yanny, B., & Brinkman, J., 2004, *AJsubmitted*, astro-ph/0410416
- Zhang, Q., & Fall, S.M., 1999, *ApJ*, 527, 81

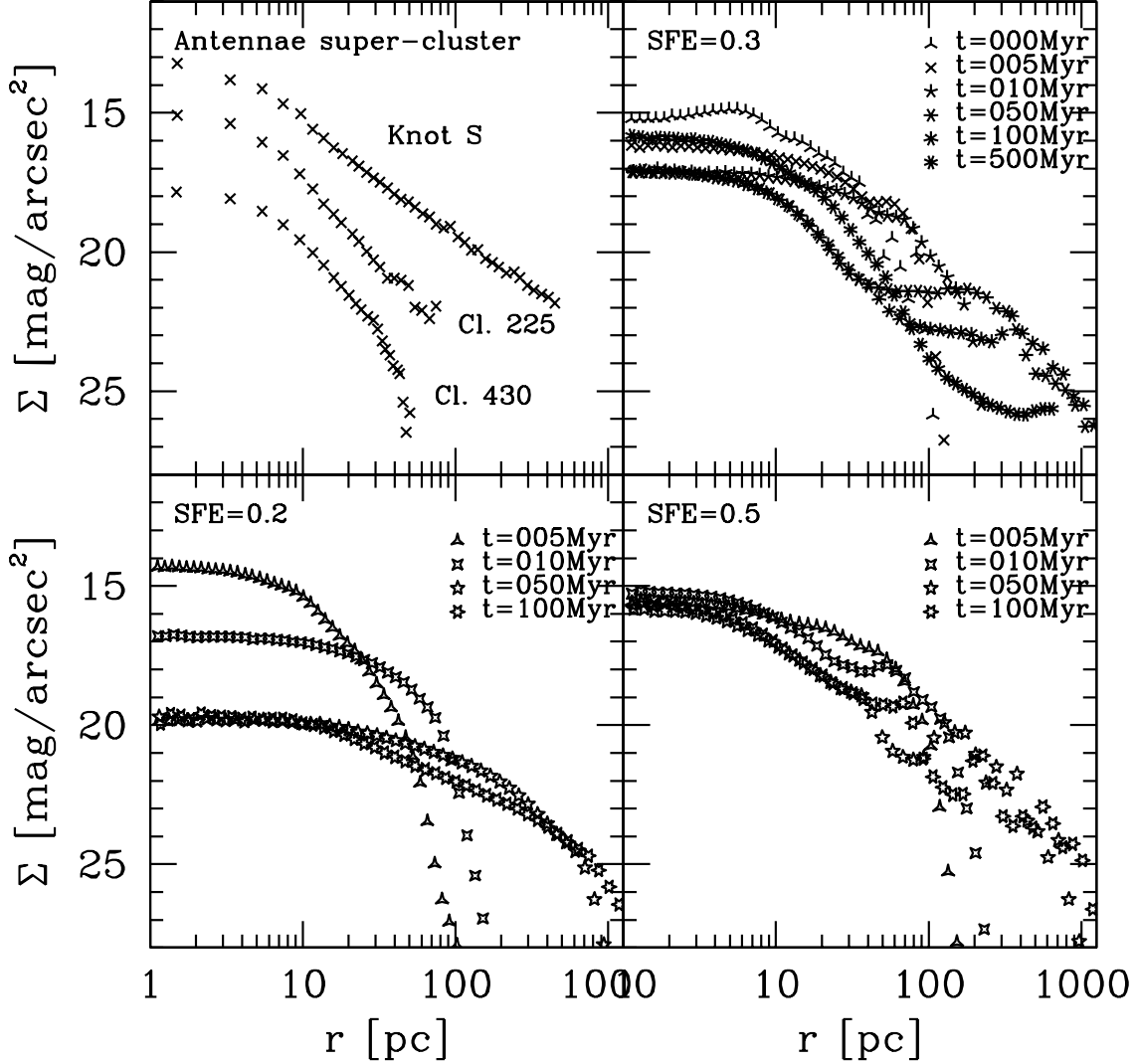


Fig. 1.— Surface-brightness profiles. Upper left: Star cluster complexes in the Antennae. Knot S and Cluster 225 are young (age < 10 Myr), while Cluster 430 is of intermediate age (a few 100 Myr). Data are taken from Whitmore et al. (1999). Upper right: Model star cluster complex or merger object, respectively, with a SFE of 0.3 (coeval) at different times. The bumps and wiggles in the profile at $t = 0$ are due to the individual star clusters. Also visible is the decrease and later increase again of the central brightness. This is due to the fact that the complex and the merger object first expands and the bound mass later contracts again. Lower left: Model star cluster complex or merger object, respectively, with a SFE of 0.2 (delayed). Here the merger object stays at a low brightness with an extended core. Lower right: At a SFE of 0.5 (coeval) almost no change in the central profile is found. In all cases the merger object fills its tidal radius at later times.

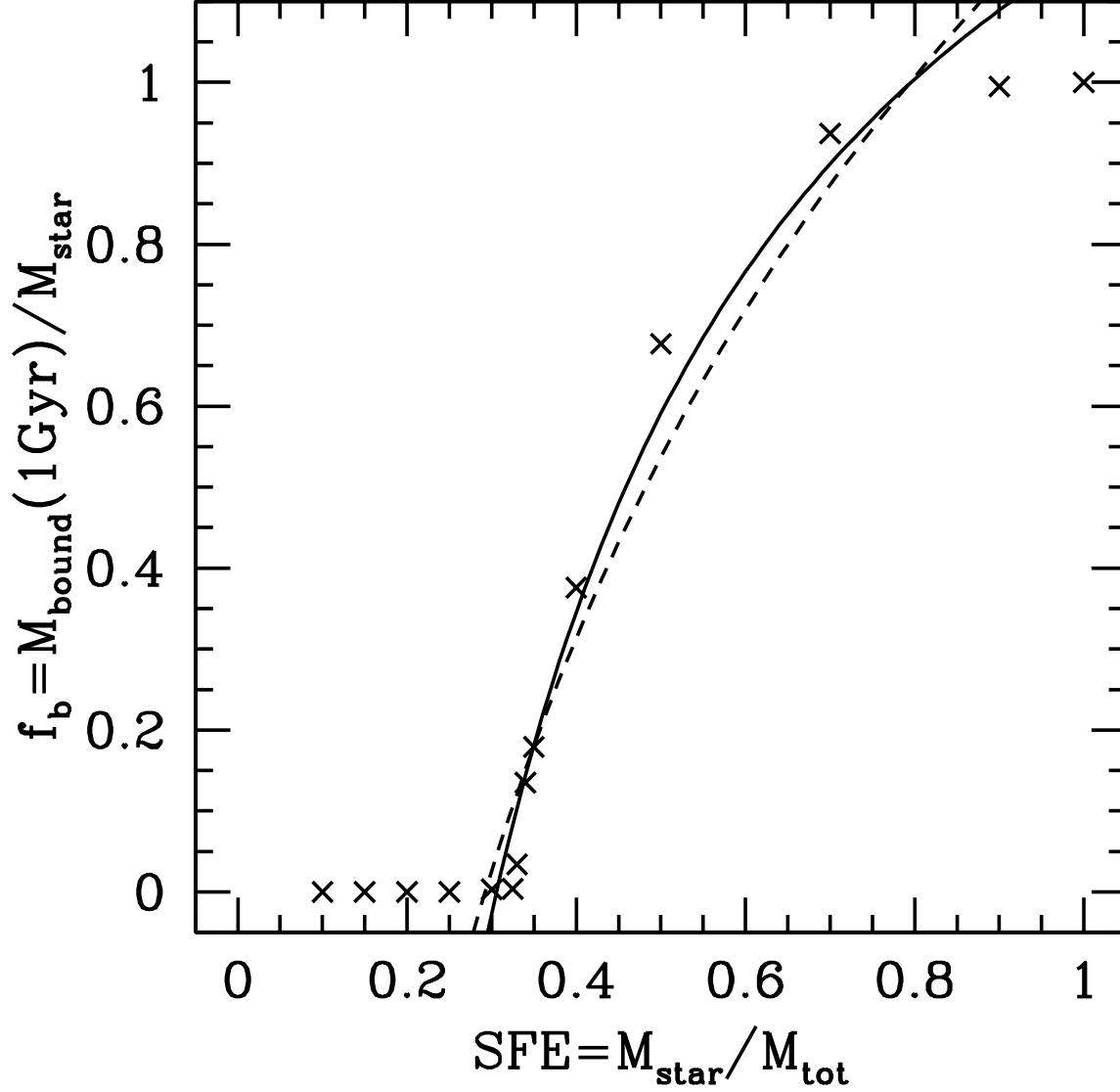


Fig. 2.— Results of the isolated cluster simulations. Plotted is the bound mass at $t = 1$ Gyr divided by the initial mass in stars against the star formation efficiency (SFE) which is the initial mass in stars divided by the total mass, i.e. the mass in stars and gas. Solid line is a power law fit: $f_b = -\text{SFE}^{-0.65} + 2.16$; dashed line is a logarithmic fit: $f_b = \ln(\text{SFE}) + 1.23$. Only the rising part ($0 < f_b < 1.0$) is fitted.

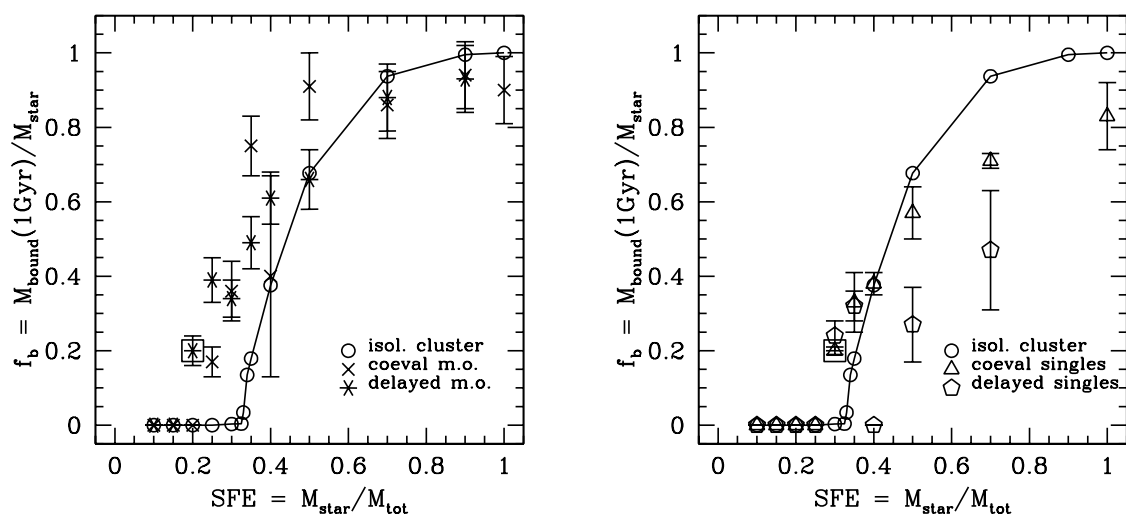


Fig. 3.— Results of star cluster complex simulations. Large open circles show the results of the isolated clusters (Fig. 2). Crosses are the merger objects of the simulations with coeval gas-expulsion, six-pointed stars denote the merger objects in the simulations with randomly delayed gas expulsion. Small open triangles and small open pentagons are surviving, escaped star clusters in the coeval and the delayed case respectively. Data points within a large open square denote the models discussed in detail in this paper.

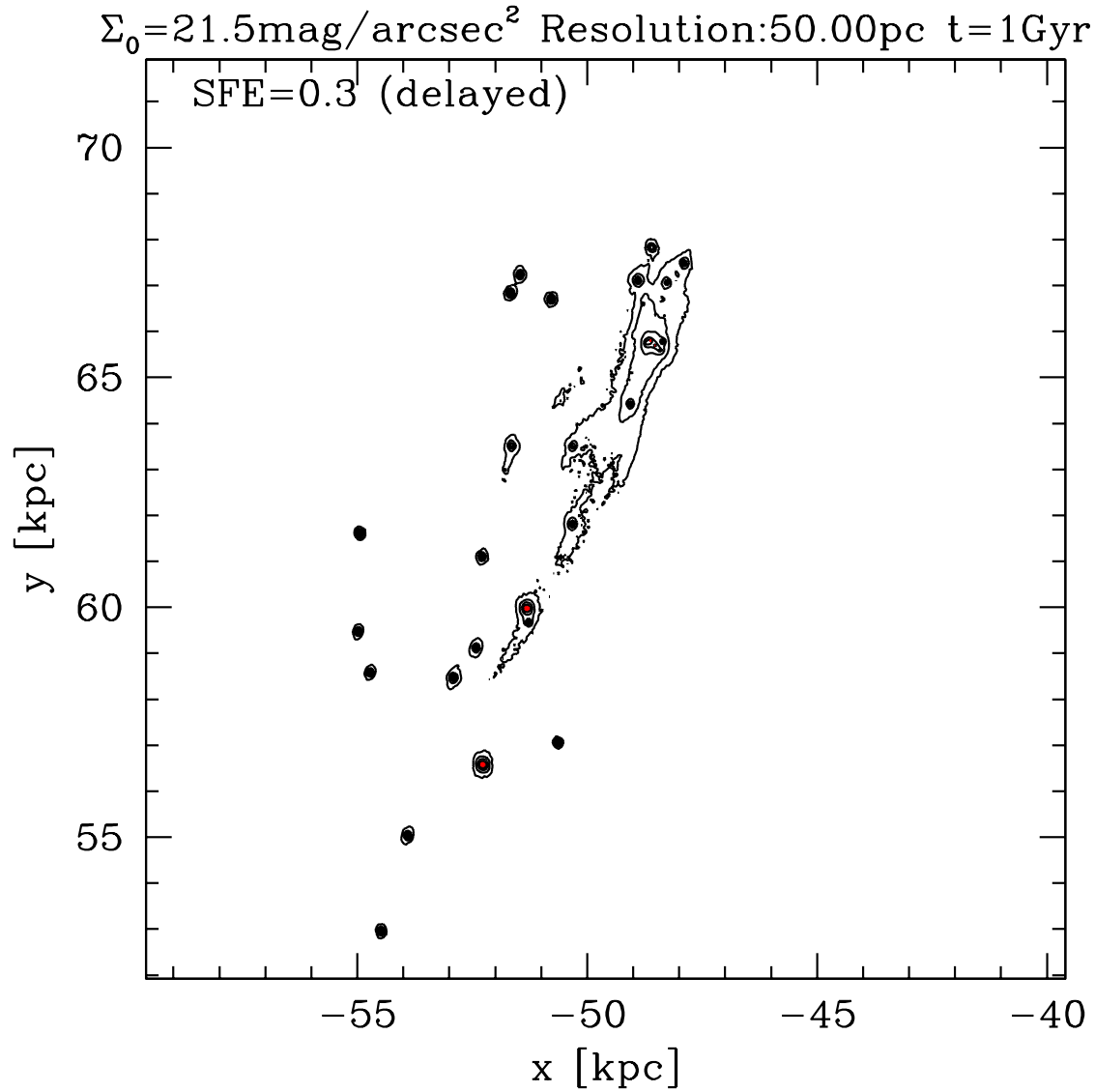


Fig. 4.— Comparison simulation with a very extended star cluster complex (effective radius = 250 pc) in the outer halo. The SFE is 30 per cent and the gas-expulsion is delayed. Shown in the figure is the surface brightness contours of the dispersed star cluster complex at $t = 1 \text{ Gyr}$ (adopting a mass-to-light ratio of 1). The surviving single star clusters are clearly visible.

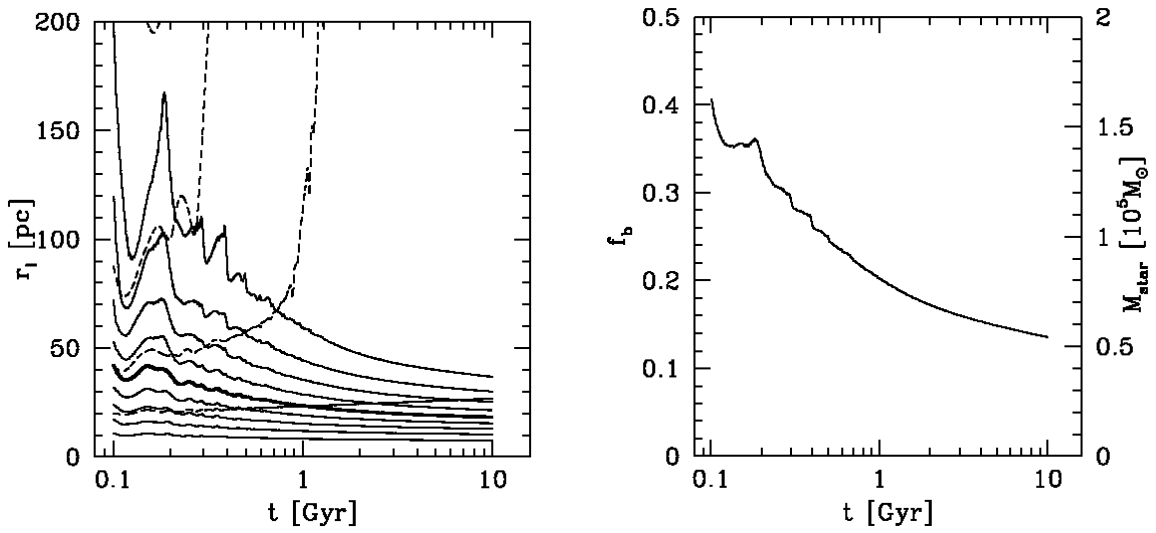


Fig. 5.— Merger object at a SFE of 20 per cent (delayed). Left: Lagrangian radii (10%, 20%, ..., 90%) of all particles (dotted) and the bound particles only (solid). Thick line is the half-mass radius. Right: Fraction of the particles which form a bound object. Right vertical axis shows the mass. We use an unusual logarithmic time-axis in both panels to enhance the evolution during the first few hundred Myr.

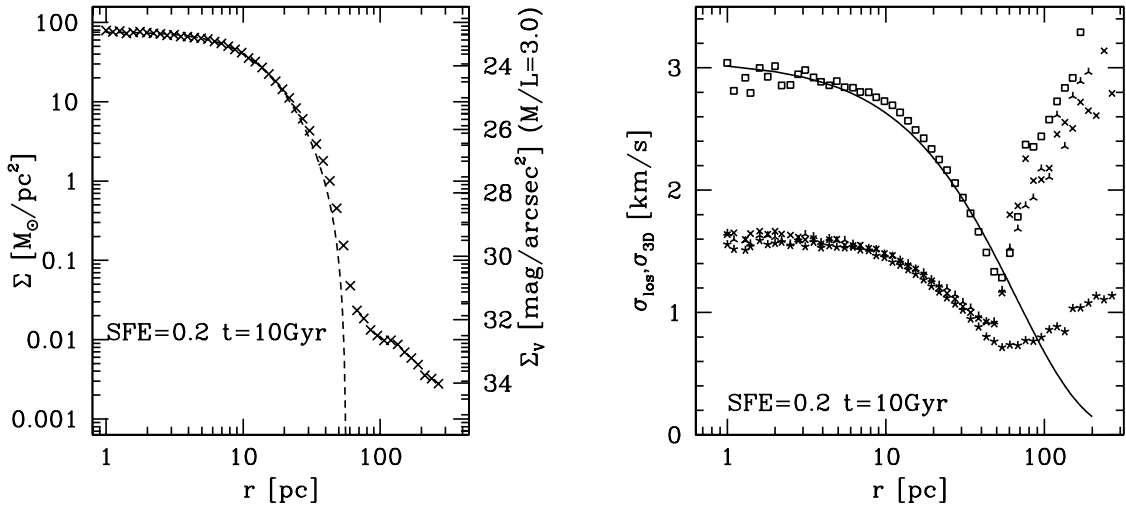


Fig. 6.— Merger object at a SFE of 20 per cent after 10 Gyr of evolution. Left: Surface density profile. Crosses are the data points and the solid line is a King profile fit as described in the main text. Right: Velocity dispersions: Tripods, crosses and 5-pointed stars are the line-of-sight velocity dispersions measured in concentric rings around the object in the directions of the x -, y - and z -axis respectively. Open squares are the 3D-velocity dispersion measured in spherical shells centred on the object. Solid line is an exponential fitting curve as described in the main text.

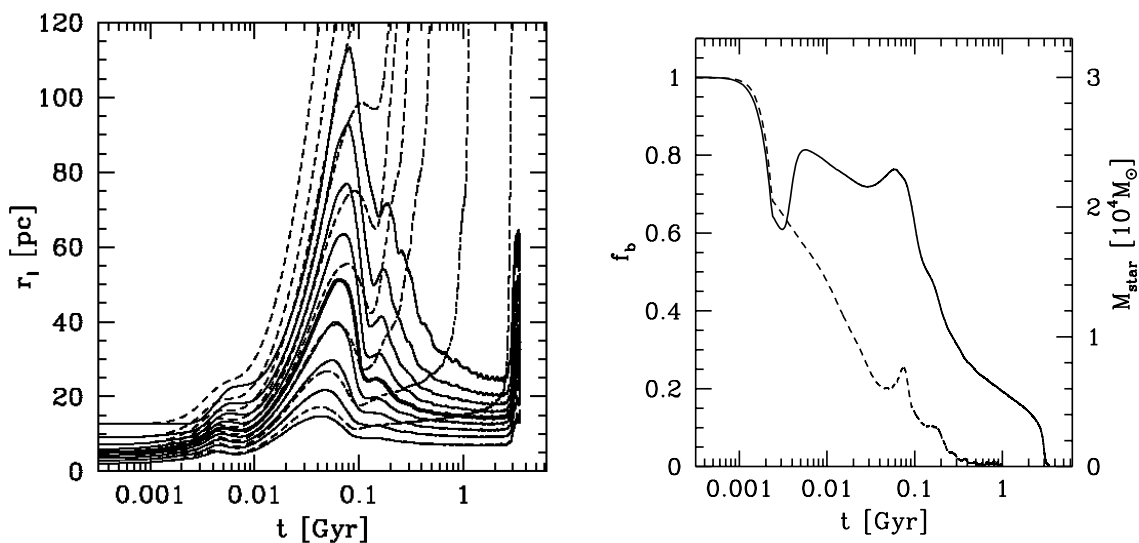


Fig. 7.— Surviving star cluster at a SFE of 30 per cent. Left: Lagrangian radii (10%, 20%, ..., 90%) of all particles (dashed lines) and the bound particles only (solid lines). Thick line denotes the half-mass radius. In this figure the turning point after which the remaining bound particles contract again is clearly visible. Right: Bound mass fraction of the surviving star cluster (solid line) and for comparison the bound mass of an isolated star cluster with the same SFE (dashed line). Clearly visible is the rise in the bound mass after 3 Myr when the star cluster gets kicked out of the cluster complex. Right vertical axis denotes the mass. To highlight the crucial evolution during the first few Myr we use time-axes that are logarithmically spaced in both panels.

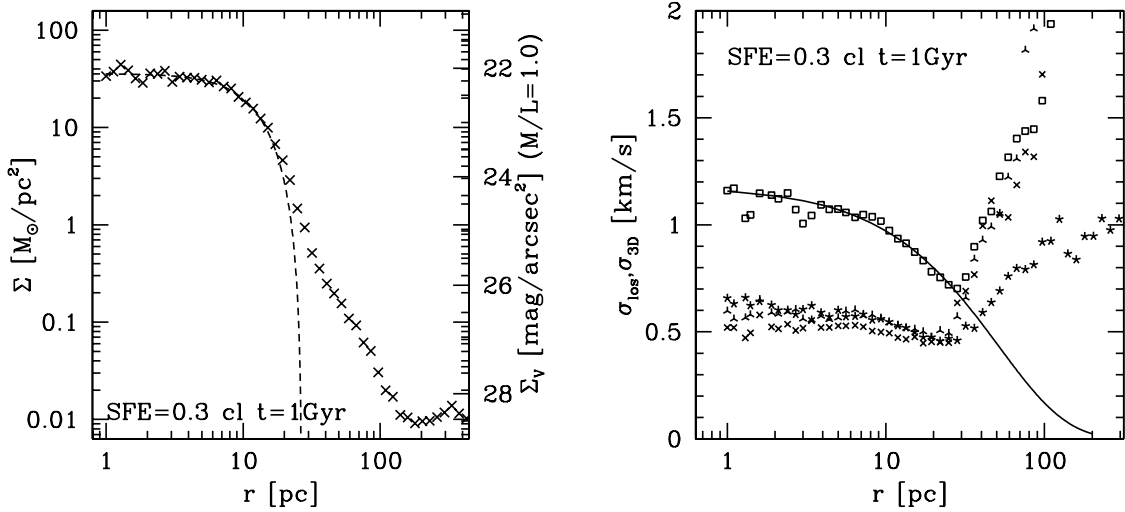


Fig. 8.— Surviving star cluster at a SFE of 30 per cent. Left: Surface density profile of a surviving star cluster with a SFE of 30 % after 1 Gyr. Crosses are the data points and dotted line is a King profile fit with a core radius of 20.6 pc and a tidal radius of 26.8 pc. Outside the tidal radius the shape is a power-law. Right: Velocity dispersions; Three pointed stars, crosses and five pointed stars are the line-of-sight velocity dispersions measured in concentric rings around the centre of the object along the x , y - and z -axis. Open squares are the 3D-velocity dispersion measured in concentric shells.

Table 1: Bound mass in per cent after 1 Gyr of evolution. SFE denotes the fraction of mass converted into stars; f_b denotes the fraction of stars remaining bound after 1 Gyr.

SFE	0.100	0.200	0.300	0.325	0.330	0.340
f_b	0.00	0.00	0.00	0.00	0.03	0.14
SFE	0.350	0.400	0.500	0.700	0.900	
f_b	0.18	0.38	0.68	0.94	1.00	

Table 2: Results from the star cluster complex simulations. M denotes the number of merged clusters, D the number of dissolved clusters, and S the number of surviving (unmerged) clusters; f_b^S denotes the bound mass fraction of the surviving clusters (if any, otherwise zero) and f_b^M denotes the bound mass fraction of the merger object. If more than one object of either kind is present the numbers denote the mean value.

SFE	coeval					delayed				
	M	D	S	f_b^S	f_b^M	M	D	S	f_b^S	f_b^M
0.10	0	20	0	0.00	0.00	5	15	0	0.00	0.00
0.15	7	13	0	0.00	0.00	10	10	0	0.00	0.00
0.20	3	17	0	0.00	0.00	12	8	0	0.00	0.20
0.25	7	13	0	0.00	0.17	14	6	0	0.00	0.39
0.30	13	5	2	0.20	0.36	12	7	1	0.24	0.34
0.35	14	3	3	0.33	0.75	10	8	2	0.32	0.49
0.40	14	3	3	0.38	0.40	13	7	0	0.00	0.61
0.50	19	0	1	0.57	0.91	15	3	2	0.27	0.66
0.70	18	0	2	0.71	0.86	17	1	2	0.47	0.88
0.90	20	0	0	–	0.94	20	0	0	–	0.93
1.00	19	0	1	0.83	0.90	–	–	–	–	–